

Automated Detection of Hypertension and Stroke by Nicking Quantification in Retinal Images

V. Meenakshi¹, Y. Syed Sha Muhammed²

¹Student, ²Associate Professor, National College of Engineering, Tirunelveli, Tamil Nadu, India.

Abstract— Retinal blood vessels morphology have been shown to be highly related to the risk of cardiovascular diseases such as hypertension, stroke and coronary heart diseases. Measuring the width of arteries and veins shown to have good correlation with the detection of cardiovascular diseases. In this paper, the true vessels in retinal images are identified as a post processing step to segmentation. The segmented vascular structure was modeled as a vessel segment graph. The blood vessels are identified by finding the forest in the graph by using the algorithm traverse. The artery vein classification method finds the arteries and veins in the retinal images. The widths of arteries and veins are measured to find the presence of hypertension and stroke. The results are analyzed and experimented with respect to actual measurements of vessel morphology. The results shows that the proposed approach is able to achieve 98.9% pixel precision and 98.7% recall of the true vessels for clean segmented retinal images, and remains robust even when the segmented image is noisy.

Keywords— Crossover point detection, Ophthalmology, retinal image, vessel width measurement, Cardiovascular diseases.

I. INTRODUCTION

Cardiovascular diseases such as stroke and coronary heart disease are the leading causes of morbidity and mortality worldwide. The state of the retinal vessel has been shown to reflect the cardiovascular condition of the body. Retinal blood vessel morphology can be an important indicator for diseases such as diabetes, hypertension, and arteriosclerosis. The central retinal artery equivalent (CRAE) and central retinal vein equivalent (CRVE) are the measurements of diameters of six arteries and veins in the retinal images. These measurements are found to have good correlation with cardiovascular diseases. However, they require the accurate extraction of distinct vessels from a retinal image. This is a challenging problem due to ambiguities caused by vessel bifurcations and crossovers.

The vascular structure consists of landmark points such as bifurcations and crossovers. A crossover is the place where two vessels cross each other while a branching or a bifurcation is the place where one vessel splits into two vessels.

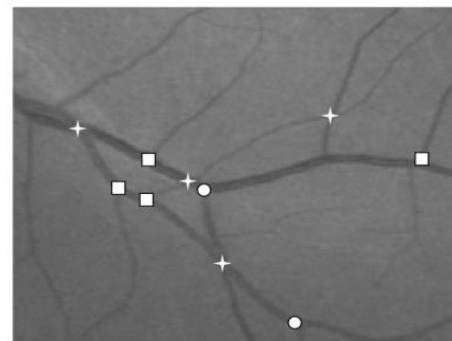


Fig.1 Example of bifurcations and crossovers. The square box indicates the bifurcations and star indicates the crossovers of blood vessels.

Fig.1 shows an example of retinal image with bifurcations and crossovers. The crossovers are often mistaken as bifurcations leading to wrong vessel identification. The square boxes denotes the bifurcations and star denotes crossovers. In order to disambiguate between vessels at bifurcations and crossovers, we need to figure out if linking a vessel segment to one vessel will lead to an adjacent vessel being wrongly identified. If vessels are incorrectly identified it leads to a large difference in the measurements. Considering multiple vessels simultaneously, information from other vessels can be used to avoid mislinking of blood vessel segments. The detection and measurement of retinal blood vessels can be used to quantify the severity of disease, as part of the process of automated diagnosis of disease or in the assessment of the progression of therapy.



International Journal of Recent Development in Engineering and Technology

Website: www.ijrdet.com (ISSN 2347 - 6435 (Online)), Volume 2, Special Issue 3, February 2014)

International Conference on Trends in Mechanical, Aeronautical, Computer, Civil, Electrical and Electronics Engineering (ICMACE14)

Thus, a reliable method of vessel detection and quantification would be valuable.

In this paper, we describe a novel technique that utilizes the global information of the segmented vascular structure to correctly identify the blood vessels in the retinal images. We model the segmented vascular structure as a vessel segment graph and transform the problem of identifying true vessels by finding an optimal forest in the graph. An objective function to find the forests is designed based on minimum cost information. After the identification of blood vessels artery vein classification was performed to distinguish artery from the veins. The widths of arteries and veins are calculated to compute the presence of hypertension and stroke. Our proposed solution employs candidate generation and expert knowledge to prune the search space. We demonstrate the effectiveness of our approach on a large real-world dataset of 2446 retinal images. The proposed technique has been incorporated as part of the semiautomated Singapore Eye Vessel Assessment(SIVA) system that has been used in real-world studies in both the community and hospital-based patient populations.

II. PRIOR WORK

The method overcomes the problems of initialization and vessel profile modeling and automatically tracks fundus vessels using linguistic descriptions like vessel and nonvessel[10]. These methods require the start points of vessels to be predetermined. Each vessel is tracked individually by repeatedly finding the next vessel point with a scoring function that considers the pixel intensity and orientation in the vicinity of the current point in the image. Tracking one vessel at a time does not provide enough information about disambiguating vessels at bifurcations and crossovers.

Automatic measurement of blood vessel tortuosity is a useful capability for automatic ophthalmological diagnostic tools. A suite of automated tortuosity measures for blood vessel segments extracted from retinal images are described [9]. The segmentation algorithm used affects the tortuosity of blood vessels by breaking vessels with high tortuosity and smooths out thin vessels. A semi-automatic method was used to measure and quantify geometrical and topological properties of continuous vascular trees in clinical fundus images [4].

It needs more user interaction to find the starting points of the retinal blood vessels. A fuzzy algorithm for vessel tracking estimates full vessel parameters, overcomes initialization and profile modeling and handles junctions of vessels in retinal images [8]. The diameter of blood vessels are measured on a two-dimensional difference of Gaussian model, which is optimized to fit a two-dimensional intensity vessel segment and does not address the other stages involved in the diagnosis of cardio vascular diseases based on vascular pathology [7].

The use of a specific model for vessel branch points and crossovers leads to more accurate and repeatable estimation of these locations and their signatures. The ERPR technique leads to significantly higher probability of successful registration on the first attempt, improving the reliability as well as the overall speed of referencing. The method increases the time of computation and computationally expensive as it includes more pixel processing [3].

The starting points of vessels are detected using a matched Gaussian filter. The detected vessels are traced with the help of a combined Kalman filter and Gaussian filter. For those vessels whose starting points are missed, the method allows the manual input by human graders. The limitation of this method is it is more accurate for the vessel profile in the retinal images only for large vessels [6].

A technique for vessel enhancement in retinal images that is capable of enhancing vessel junctions in addition to linear vessel segments was used. The approach does not use vessel connectivity constraints so it is possible to use it as a pre-processing stage before employing known algorithms that do use vessel connectivity constraints and so improve their performance [2]. A method that combines color change information and image understanding systems outputs in a novel manner is used to analyze vascular changes such as increase or decrease in width, and disappearance or appearance of vessels [5]. Al-Diri *et al.* [1] used expert rules to resolve vessel crossovers and locally linked up segments at these crossovers to give a vascular network. However, they did not identify complete vessels. Our work is focused on the detection of blood vessels as a post processing step to segmentation.

We identify multiple vessels simultaneously and use global structural information to figure out if linking a vessel segment to one vessel will lead to an overlapping or adjacent vessel being wrongly identified. After identification of blood vessels we perform the classification of arteries and veins. We calculate the widths of arteries and veins to detect the presence of hypertension and stroke.

III. METHODOLOGY

A. Preliminary Steps

We define the zone of interest in the retinal image. This is a circular ring bounded by concentric circles of radii $2r$ and $5r$ where r is the radius of the optic disc (OD).

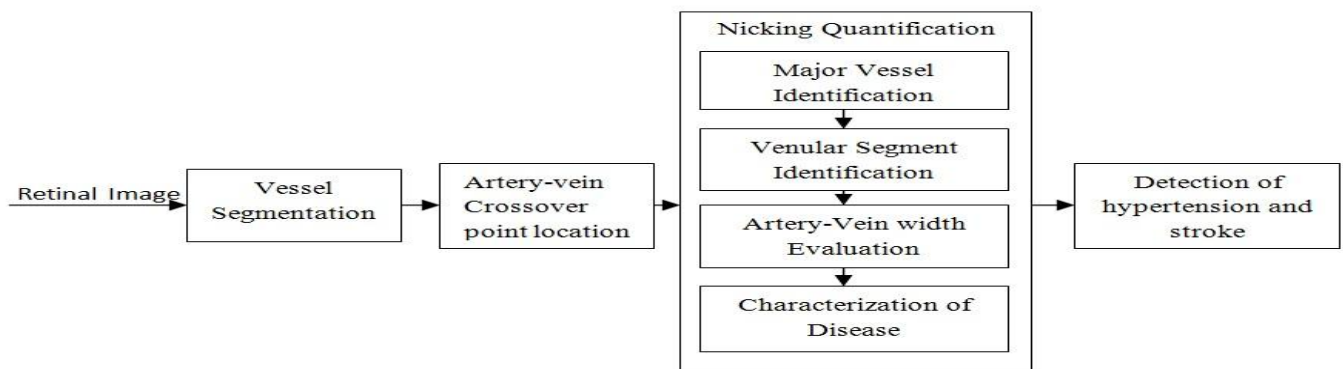


Fig.2 Steps of the proposed nicking quantification for the detection of hypertension and stroke.

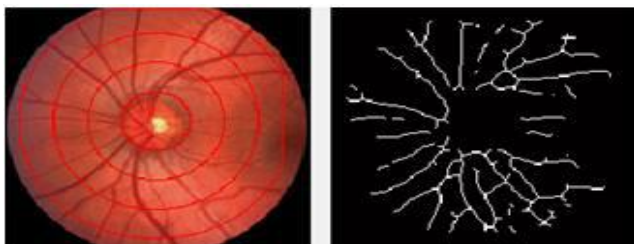


Fig.3(a) Zone of interest and vessel structure. (b) Line image of vascular structure.

The main steps involved in the detection of cardiovascular diseases was shown in the Fig.2. The zone of interest was defined as shown in the Fig. 3(a). Each vessel starts from the pixel near the circle of radius $2r$. The pixels are called root pixels. We utilize existing vessel segmentation methods and apply any skeletonization procedure to obtain the line image in the zones of interest [see Fig. 3(b)]. The lines in the line image depict the topological connectivity of the vessel structures.

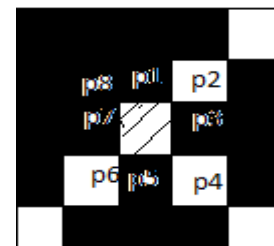


Fig. 4 Example Junction pixels.

Let P be the set of all white pixels in a line image. Two pixels $p_i, p_j \in P$ are adjacent, i.e., $\text{adj}(p_i, p_j)$, if and only if $p_j \in \text{neigh8}(p_i)$, where $\text{neigh8}(p) = \{p_1, p_2, \dots, p_8\}$ is the eight neighbourhood of p [see Fig. 4].

Definition-1 (Connected Pixels): Pixels $p_i, p_j \in P$ are connected, i.e., $\text{conn}(p_i, p_j)$, if $\text{adj}(p_i, p_j)$ or $\exists p_c \in P - \{p_i, p_j\}$ s.t $\text{conn}(p_i, p_c) \wedge \text{conn}(p_c, p_j)$.

Definition-2 (Pixel Crossing Number): Let p_1, \dots, p_8 be a clockwise sequence of the eight neighbour pixels of pixel p . Then, $x_{\text{num}}(p)$ is the number of black to nonblack transitions in this sequence of neighbour pixels of p .

Definition-3 (Junctions): Let $white8(p) \subseteq neigh8(p)$ be the set of white pixels that are neighbors of p . The set of junction pixels in P is $YP = \{p \in P | xnum(p) > 2 \vee pixels, i.e., J \subseteq YP \text{ such that } \forall pi, pj = i \in J, conn(pi, pj), \text{ where } conn \text{ is restricted to the set } YP. \text{ Then, the set of all junctions in } P \text{ is } JP. \text{ Fig. 3 depicts the examples of Junction pixels. In Fig. 3(a), we have } white8(p) = \{p2, p4, p6\}, \text{ and } xnum(p) = 3 \text{ due to the transitions } (p1, p2), (p3, p4) \text{ and } (p5, p6). \text{ This is the case where the shaded pixel } p \text{ is the junction pixel with } xnum(p) > 2.$

Definition-4 (Segment): A segment s is a sequence of unique white pixels $p1...pn$ in P such that all of the following conditions are true:

- 1) $n > 0$ and $\forall i \in [1, n], pi \in JP.$
- 2) $n > 1 \Rightarrow \forall i \in [1, n-1], adj(pi, pi+1).$
- 3) $\forall i \in \{1, n\}, |white8(pi)| = 1 \vee \exists pj \in JP \text{ s.t. } adj(pi, pj)$
- 4) $n > 2 \Rightarrow \forall i \in [2, n-1], xnum(pi) = 2.$

We define $p1$ and pn be the end pixels of s . Let SP be the set of all segments in P and $NP = P - YP, i.e., NP$ contains nonjunction pixels that are part of segments. Then, $s \in SP$ is adjacent to a junction $J, i.e., adj(s, J), \text{ if } \exists pj \in J \text{ s.t. } adj(pj, p1) \vee adj(pj, pn).$ Consequently, two segments $sa, sb \in SP$ are adjacent $adj(sa, sb)$ if $\exists J \in JP \text{ s.t. } adj(sa, J) \wedge adj(sb, J).$

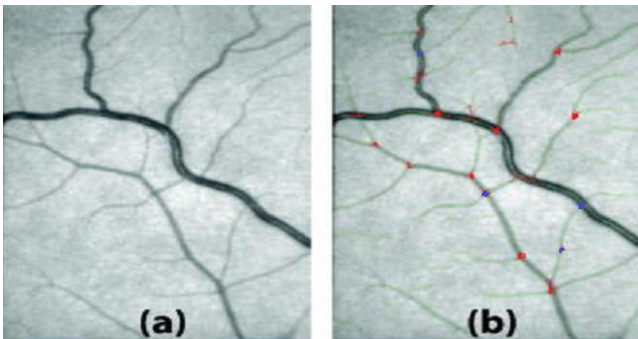


Fig. 5(a)segments (b)bifurcations points shown in red colour and junctions shown in blue colour.

Fig. 5 shows the examples of segments and junction pixels according to Definitions 3 and 4 for a region from a line image. The bifurcations are denoted in red and junctions in blue.

B. Crossover Locations

To detect the crossover points, the vascular skeleton and edge images are first extracted from the segmented image using binary operations. The vessels skeleton is extracted using thinning process which successively erodes away pixels on the boundary of the objects while preserving its connectivity until no more thinning is possible. The vessel edge image is achieved by a morphological operator which removes interior pixels and retains only pixels on the vessel boundaries. The crossover locations are then detected by extensive analysis on the extracted vascular skeleton and edge images as follows. At each skeleton pixel P , we compute the cross-point number (cpn) as follows:

$$Cpn(p) = \frac{1}{2} \sum_{i=1}^8 |N_i(P) - N_{i+1}(P)| \quad (1)$$

Where $N_i(P)$ are the neighbour pixels of P named in an anti-clockwise order and $N9(P) = N1(P).$

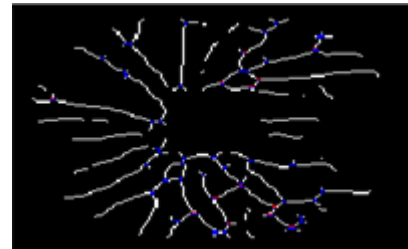


Fig 6. Crossover points in blue and crossover segments in red.

The cpn number computed for each skeleton pixel represents the number of vessel segments connected to that pixels with cpn equal to 3 are initially marked as bifurcation candidate while those with cpn equal to 4 are labelled as crossover candidates. Then, two bifurcation candidates are further grouped as one crossover if they are connected by at most T pixels. The segment that connects the two bifurcation point is then identified and its middle point is located and served as the true position of that crossover. This step helps to detect crossover points that are represented by two bifurcation points in the skeleton image when two vessels intersect at an acute angle.



International Journal of Recent Development in Engineering and Technology

Website: www.ijrdet.com (ISSN 2347 - 6435 (Online)), Volume 2, Special Issue 3, February 2014)

International Conference on Trends in Mechanical, Aeronautical, Computer, Civil, Electrical and Electronics Engineering (ICMACE14)

C. Vessel Identification

After finding the crossover points, we model the segments as a segment graph and use constraint optimization to search for the best set of vessel trees from the graph.

Definition-5(Segment Graph): Given the set of white pixels P in a line image, a segment graph $G_p=(S_p,E_p)$, where each Vertex in S_p is a segment and an edge $e_{i,j}=(s_i,s_j) \in E_p$ exists if $adj(s_i,s_j), s_i,s_j \in S_p, i \neq j$. Typically, G_p consists of disconnected subgraphs that are independent and can be processed in parallel. We refer to each of these subgraphs as the segment G_p . The goal is to obtain a set of minimum cost trees from the segment graph such that each minimum cost tree corresponds to a vessel in the retinal image.

Definition-6(Vessel): Given a segment graph $G_p=(S_p,E_p)$, a vessel is a tree, $T=(s_{root},V_T,E_T)$ such that S_{root} is the root node, $root(T)=s_{root}, V_T \subseteq S_p$ and $E_T \subseteq E_p$. A set of such trees is called a forest. Here the forest is the combination of minimum spanning tree and binary search tree. Segment end points near the inner circle of the zone of interest are identified as root pixels. The root of each tree corresponds to the root segment that contains a unique root pixel.

In minimum spanning trees, edges with minimum costs are traversed and in binary search trees left node has the minimum cost. We formulate the goal of simultaneous identification as a constraint optimization problem (COP). The entire tree structure was modelled as a minimum cost forest consisting of minimum spanning trees and binary search trees.

Given a segment graph $G_p=(S_p,E_p)$ and a set of root segments S_{root} , let F_p be the set of all possible forests from G_p for each root segment in S_{root} . The optimal forest, $F \in F_p$, that corresponds to vessels in G_p is given by

$$F = \underset{F \in F_p}{\operatorname{argmin}} \operatorname{cost}(F) \quad (2)$$

The trees are subjected to the following constraints:

- 1) Roots are unique to each tree.
- 2) The directional change between the segments are within the threshold of 135° .

- 3) Any segment appearing in more than one segment must be a crossover segment.
- 4) Any parent segment at the crossover segment must connect to the child with minimum directional change.
- 5) Crossover segment is the only child and have only one child that has the minimum directional change.
- 6) Leaf segments cannot be crossover segments.

In addition to the above constraints, each segment may not appear twice and should not form cycles. Our cost function makes use of change in direction between segments. For a vessel T let the set of bifurcations be

$$Y_T = \{ (s_y, s_1, s_2) / s_y, s_1, s_2 \in V_T \wedge (s_y, s_1), (s_y, s_2) \in E_T \} \quad (3)$$

$\Gamma Y(T)$ sums the average of the parent child directional changes at bifurcations. $\Gamma I(T)$ sums the change in direction between parents in tree with only one child segment. This favours small direction between parents in when choosing between segments to connect at segments to connect at Junctions. Finally the cost function of the forest defined assumes the parent-child directional change in the bifurcations in T . Finally the cost function of the forest was defined as,

$$\operatorname{Cost}(F) = \sum_{T \in F} [\Gamma Y(T) + \Gamma I(T)] \quad (4)$$

Instead of defining the cost on edges we define the cost on forests to allow weighting and fusing of multiple cost criteria at the forest level. We find the forest from the connected graph.

To solve the COP, we use a candidate enumeration algorithm that utilizes the lower bound of the cost function to prune the search space. This lower bound $LB_{\operatorname{cost}}(F)$ is based on the following theorem.

Theorem(lower Bound of cost)

Given a set of trees F and any vessel $T \in F$, we construct the vessel T_- by growing one leaf node of T such that it has either one or two children. Let $F_- = F - \{T\} \cup \{T_-\}$. Then, $\operatorname{cost}(F) \leq \operatorname{cost}(F_-)$, i.e., $\operatorname{cost}(F)$ is the lower bound cost of any F_- resulting from growing the vessels in F .

Proof: By adding new children to a leaf node, we increase the size of I_T by one, Y_T by one, or neither, but not both. Thus, $\operatorname{cost}(F) \leq \operatorname{cost}(F_-)$.



International Journal of Recent Development in Engineering and Technology

Website: www.ijrdet.com (ISSN 2347 - 6435 (Online)), Volume 2, Special Issue 3, February 2014)

International Conference on Trends in Mechanical, Aeronautical, Computer, Civil, Electrical and Electronics Engineering (ICMACE14)

Algorithm: Traverse

```
Input: Gp={Sp,Ep},Sroot
Output: Fmin
1:C ← set of constraints (1)-(6) in COP formulation
2:F[1..n] ← (vessels of root nodes in Sroot)
3:R[1..n] ← (root(F[T]) for T ∈ [1..n])
4:cmin ← ∞; Fmin ← F[] #root node vessels
5:Traverse(1,F,R)
6:return Fmin
Procedure Traverse(I,F,R)
7:if cost(F)<cmin ∧ F cannot be grown without violating C
then
8: cmin ← cost(F); Fmin ← F
9:else if LBCost(F) ≤ cmin then
10: for T=i to n do
11: while R[T] ≠ ∅ do
12: sT ← pop(R[T]) #valid children of sr forward checking
13: N ← FindChildren(F,sT) #left and right pairs
14: if(outdegree==1) #minimum spanning tree
15:   Push(R[T],sT)
16:   cmin ← cost[F]; Fmin ← F;
17: elseif(outdegree>1) #binary Search tree
18:   for each (sl,sr) ∈ N do
19:     left(sT) ← sl;
20:     cmin ← cost[F]; Fmin ← F;
21:     Push(R[T],sl);
22:     Traverse(T,F,R)
23:   endfor
24:   Pop(R[T]) #Pop sl
25:   endif
26:   left(sT) ← ∅; right(sT) ← ∅ #Proceed until end pixel
reached
27:   end while
28:   end for
29:   end if
```

Fig.7 Details of the algorithm Traverse.

Fig. 7 shows the details of the algorithm Traverse. It detects the blood vessels by combination of minimum spanning tree and binary search tree. The input is the segment graph with n root segments given in Sroot. Lines [1]-[6] initializes the global variables where F[1..n] denotes the initial forest of n vessels. R[1..n] denotes the stack for each vessel. cmin denotes the minimum cost and the Fmin represents the minimum cost forest.

In Traverse, if forest F satisfies all the global constraints and cannot be grown further then we update Fmin if $\text{cost}(F) < \text{cmin}$. Otherwise we may proceed the growth of the forest F with the lower bound $\text{LBCost}(F)$. The outer loop at line 10 orders each vessel T ranges from current index i to n ensuring T includes only the original forest. Stack stores all of the current leaf nodes to be grown and to enumerate vessels in a lower cost edge traversal.

A subprocedure *findchildren* returns pairs (sl,sr) of possible children for the current node s_T. If only one child is to be added, we traverse in minimum cost approach. *findchildren* employs forward checking to eliminate children pairs that violate constraints (1)-(6) in COP formulation. If there are more than one child for a node binary search tree is used where only left child consists of lowest cost. The blood vessels are continuously traversed in combination of minimum spanning tree and binary search tree. Fig. 8 shows the result of applying traversal in the segment graph.

The time complexity of the algorithm traverse is exponential to the cost of edges and independent on the size of the retinal image. It deals only with the connectivity and not in pixel properties such as intensity. The Traverse extracts all the blood vessels without any mislinking of adjacent blood vessels.

D. Venular Segment Identification

The simplified segmentation provides us with a vascular network containing four segments, two associated with the vein and two associated with the artery. Our analysis is performed on the vein, therefore we need to determine which pair is associated to the vein. This is done by an analysis on the vessel skeleton and edge images extracted from the simplified segmentation.

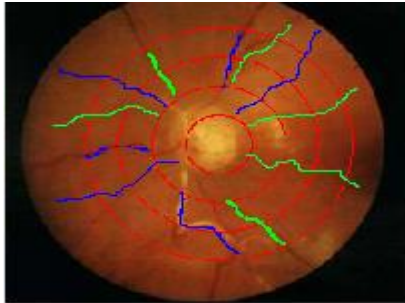
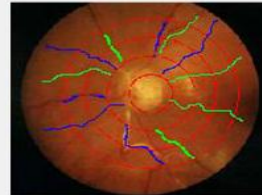


Fig 8. Finding Optimal forest from the algorithm traverse and classification of arteries and veins



Arteries width—>94

Veins width—>82

Presence of Hypertension

Fig. 10 Artery vein width evaluation and detection of hypertension.

Hence, the color information of the two vessels is computed and the artery is assigned to the vessel with higher intensity value. Different color spaces, RGB and HSV as well as the gray level, were used to identify the most discriminative feature. The median intensity value of each vessel is computed as:

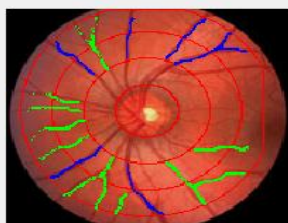
$$Fvssi = \text{median}(X(VSS_i)) \quad (5)$$

Where $i \in \{1, 2\}$, $X \in \{R, G, B, H, S, V, \text{Grey}\}$ representing colour components. For example, $R(VSS_1)$ contains the intensity values of the red channel of the first vessel. Then the vein is identified as the vessel with lower intensity level. Once the vein is correctly identified its segments are extracted for subsequent analysis.

E. Artery vein width Evaluation

The vessel measurements CRAE, CRVE have been found to have good correlation with risk factors of cardiovascular diseases and are positive real numbers. CRAE and CRVE are computed by iteratively by combining the mean widths of consecutive pairs of vessels in major arteries and veins respectively as follows:

$$\begin{aligned} \text{Arteries: } \hat{w} &= 0.88.(w_1 + w_2)^{1/2}. \\ \text{Veins: } \hat{w} &= 0.95.(w_1 + w_2)^{1/2}. \end{aligned} \quad (6)$$



Arteries width—>124

Veins width—>140

Presence of Stroke

Fig. 9 Artery vein width evaluation and detection of stroke.

The classification process is then performed to distinguish the vein from the artery. For the majority of crossover points, it is observed that the artery appears brighter than its vein counterpart. This is due to the fact that the artery contains oxygenated blood which is pumped from the heart, making it red, while the vein carries deoxygenated blood back to the heart, which makes it darker.



International Journal of Recent Development in Engineering and Technology

Website: www.ijrdet.com (ISSN 2347 - 6435 (Online)), Volume 2, Special Issue 3, February 2014)

International Conference on Trends in Mechanical, Aeronautical, Computer, Civil, Electrical and Electronics Engineering (ICMACE14)

Where w_1, w_2 are a pair of widths values and \hat{w} is the newly combined width value for the next iteration. Iteration stops when one width value remains. Fig. 9 shows the detection of cardiovascular diseases by calculating the vessel widths.

F. Characterization of diseases

One of the signs of hypertension that can be found on retinal fundus images is arteriolar narrowing. The arteriolar narrowing is often assessed by measuring the vessels widths of vessels running side by side and at a certain distance from the optic nerve head. However, such measurement is seldom done systematically and quantitatively, making the consistent evaluation difficult. Therefore, automated calculation of widths of arteries and veins in retinal fundus images can be useful to ophthalmologists in the detection of arteriolar narrowing and longitudinal evaluation of vasculature conditions. Fig.9 shows the detection of stroke by identifying width of blood vessels. Sign of stroke that can be found on retinal images is the widening of retinal blood vessels. It can be measured by calculating the width of arteries and veins. If the width is more than the normal blood vessels, the person is highly prone to be attacked by stroke. Fig. 10 shows the detection of hypertension by evaluating the width of blood vessels. The persons highly prone to hypertension suffers from arteriolar narrowing.

IV. EXPERIMENTAL RESULTS

We implement the algorithm traverse that traces all the vessels simultaneously. We evaluate the performance on both noisy and clean images. Noisy line images are obtained using an existing vessel segmentation algorithm and is representative of the real-world situation where segmentation is often imperfect. We use the following evaluation metrics based on the pixels in the entire vessels. Let Big6 refer to the six largest arteries and veins ranked by the average width of the first segment of each vessel. Further, if a pixel of a traced vessel exists in the gold standard it is called a matched pixel.

1) *Pixel precision*: Total number of matched pixels divided by total number of traced pixels.

2) *Pixel recall*: Total number of matched pixels divided by total number of gold standard pixels.

3) *Big6 precision*: Total number of matched pixels divided by total number of traced pixels of Big6.

4) *Big6 recall*: Total number of matched pixels divided by total number of gold standard pixels of Big6.

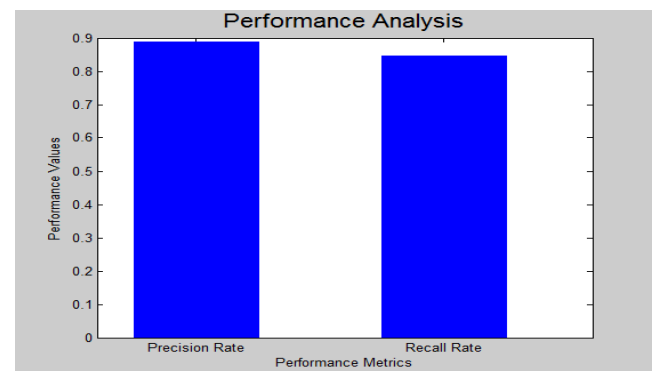


Fig. 11 Precision and Recall rate of the algorithm traverse.

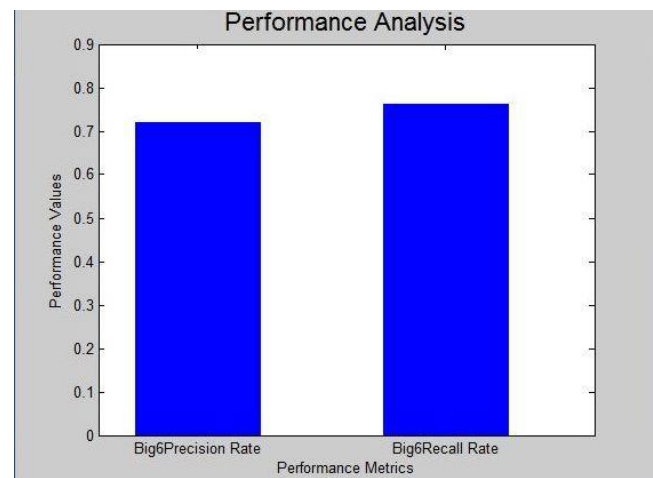


Fig. 12 Big6 Precision and Big6 Recall rate of algorithm traverse.

The traverse is able to achieve near perfect pixel precision(98.9%) and pixel recall (98.7%). Fig. 11 represents the pixel precision and recall rate of clean images when applying algorithm traverse.



Fig. 12 represents the Big6 Precision and Big6 Recall rate of clean images when applying traverse. The performance of all the tracers decrease for noisy images but traverse is more robust. The algorithm Traverse traces all the vessels simultaneously with knowledge about all other vessels.

The artery-vein classification accuracy (ACC) can be used to evaluate the performance of the system. ACC is defined as the fraction of arteries and veins correctly classified over the total number of arteries and veins.

Table I
Artery Vein Classification accuracy Colour Feature ACC (%)

Grey level	94.44
RGB Components	
Red	91.11
Green	96.67
Blue	67.68
HSV Components	
Hue	83.33
Saturation	73.33
Value	91.11

Table I shows that green channel provides highest accuracy when compared to other channels. So, green channel can be most effectively used for blood vessel extraction. The algorithm Traverse accurately traces all the vessels and more robust in the presence of noise. The measurements of veins are consistently more correlated than those of arteries, indicating that arteries are more difficult to segment than veins. The algorithm takes all the vessels into account and thus leading to better identification during bifurcations and crossovers.

V. CONCLUSION

We have proposed a technique for the accurate detection of true blood vessels and detection of cardiovascular diseases by calculating the width of arteries and veins in the retinal images. The technique was modelled as a post processing step to segmentation. The vascular structure was modelled as a segment graph and finding the optimal forest in the graph to search for the best set of vessels.

The vessels are modelled as a combination of minimum spanning tree and binary search tree. In this paper, the forward traversal was performed. In future, both the forward and reverse traversals for finding the blood vessels can be performed. For finding the reverse traversal the end pixel was considered. All blood vessels are taken into account while forming the optimal forest. It results in avoiding mislinking of blood vessels. The blood vessels are classified to distinguish the blood vessels into arteries and veins. The width of arteries and veins are calculated to detect the presence of cardiovascular diseases. The method can be extended by improving the vessel identification in noisy images.

REFERENCES

- [1] B. Al-Diri, A. Hunter, D. Steel, and M. Habib, "Automated analysis of retinal vascular network connectivity," *Comput. Med. Imag. Graph.*, vol. 34, no. 6, pp. 462-470, 2010.
- [2] Changhua Wua and Gady Agam, "Probabilistic Retinal vessel segmentation," *SPIE Medical Imaging in Image Processing*, vol. 12, no. 5, pp. 267-272, 2007.
- [3] Chia-Ling Tsai, Charles V. Stewart, Howard L. Tanenbaum and Badrinath Roysam, "Model-Based Method for Improving the Accuracy and Repeatability of Estimating Vascular Bifurcations and Crossovers From Retinal Fundus Images", *IEEE Transaction on Information Technology in Biomedicine*, vol. 8, no. 4, 2004.
- [4] M. Elena Martinez-Perez, Alun D. Hughes, Alice V. Stanton, Simon A. Thom, Neil Chapman, Anil A. Bharath, and Kim H. Parker, "Retinal Vascular Tree Morphology: A Semi-Automatic Quantification", *IEEE Transactions on Biomedical Engineering* vol. 48, no. 9, August 2002.
- [5] Harihar Narasimha-Iyer, Member, IEEE, Ali Can, Badrinath Roysam, Howard L. Tanenbaum, and Anna Majerovics, "Integrated Analysis of Vascular and Nonvascular Changes From Color Retinal Fundus Image Sequences", *IEEE Transactions on Biomedical Engineering*, vol. 54 no. 8 August 2007.
- [6] H. Li, W. Hsu, M. L. Lee, and T. Y. Wong, "Automatic grading of retinal vessel caliber," *IEEE Trans. Biomed. Eng.*, vol. 52, no. 7, pp. 1352-1355, Jul. 2005.
- [7] James Lowell, Andrew Hunter, David Steel, Ansu Basu, Robert Ryder, and R. Lee Kennedy, "Measurement of Retinal Vessel Widths From Fundus Images Based on 2-D Modeling" *IEEE Transactions on Medical Imaging* vol. 23, no. 10, October 2004.
- [8] Sina Hooshyar, Rasoul Khayati and Reza Rezai, "Vessel Tracking for Retina Images Based on Fuzzy Ant Colony Algorithm", *IEEE Transactions on Biomedical imaging* vol. 22, no. 12, 2002.
- [9] William E. Hart, M. Goldbaum, P. Kube, and M. R. Nelson, "Automated measurement of retinal vascular tortuosity," in *Proc. AMIA Fall Conf.*, pp. 459-463, 1997.



International Journal of Recent Development in Engineering and Technology

Website: www.ijrdet.com (ISSN 2347 - 6435 (Online)), Volume 2, Special Issue 3, February 2014)

International Conference on Trends in Mechanical, Aeronautical, Computer, Civil, Electrical and Electronics Engineering (ICMACE14)

- [10] Y.Tolias and S.Panas, "A fuzzy vessel tracking algorithm for retinal images based on fuzzy clustering," IEEE Trans. Med. Imag., vol. 17, no. 2, pp. 263–273, Apr. 1998.
- [11] Uyen T. V. Nguyen, Alauddin Bhuiyan, Laurence A. F. Park, Ryo Kawasaki, Tien Y. Wong, Jie Jin Wang, Paul Mitchell, Kotagiri Ramamohanarao, "An Automated method for retinal Arteriovenous Nicking Quantification from color fundus images", IEEE Transactions on Biomedical Engineering, 2013.
- [12] Qiangfeng Peter Lau, Mong Li Lee, Wynne Hsu, and Tien Yin Wong, " Simultaneously Identifying all true vessels from segmented retinal images", IEEE Transactions on Biomedical Engineering, vol. 60, no. 7, July 2013.